RSC Advances

PAPER

View Article Online
View Journal | View Issue

Cite this: *RSC Adv.*, 2025, **15**, 43595

Sludge biochar-enabled trace voltammetric detection of 2,2′,4,4′-tetrabromodiphenyl ether in water samples

Ganquan Zhang,†[a] Yuanping Li, †*[a] Shunyao Jia,†[b] Yaoning Chen, *[b] Tianyun Zhou,[a] Li Zhu,[a] Nianping Chi,[a] Yanting Wu[a] and Wenqiang Luo[a]

In this study, the conversion of municipal sludge into functional biochar modifiers enabled the construction of an ultrasensitive electrochemical interface for the quantification of trace-level 2,2′,4,4′-tetrabromodiphenyl ether (BDE-47), obviating the necessity for sample pretreatment. A novel electrochemical electrode was developed by modifying a glassy carbon electrode (GCE) with sludge biochar, and a linear equation was established for the determination of trace BDE-47 using cyclic voltammetry. Scanning electron microscopy (SEM), Brunauer–Emmett–Teller (BET) and Fourier transform infrared (FTIR) spectroscopy analyses revealed that the sludge biochar pyrolyzed at 600 °C in an oxygen-free environment formed additional pore structures with more adsorption sites. This enhanced the accuracy of the determination and improved the convenience of electrochemical detection. Additionally, factors such as the pH and scanning rate were optimized and examined. Under the optimized experimental conditions, the peak current increased linearly with the BDE-47 concentration in the range of 0.005 μg L^{-1} to 0.6 μg L^{-1}, leading to the construction of a linear curve for the assay. The detection limit was 5 ng L^{-1}, and the average recoveries ranged from 96.79% to 106.63%. Furthermore, this method was successfully applied to determine BDE-47 concentrations in real water samples, and the results were consistent with those obtained by liquid chromatography. The modified electrode established a simple yet robust voltammetric strategy for rapid BDE-47 screening in water, fulfilling the growing demand for decentralized monitoring tools for persistent organic pollutants (POPs).

Received 16th August 2025
Accepted 3rd November 2025

DOI: 10.1039/d5ra06052d

rsc.li/rsc-advances

1. Introduction

2,2′,4,4′-Tetrabromodiphenyl ether (BDE-47) is widely used as a flame retardant in various products, including electronics, textiles, furniture, and building materials, due to its ability to reduce the burning rate of materials and its low cost.[1] However, increasing researches have shown that BDE-47 may be potentially toxic to humans, leading to it being banned in many regions.[2,3] BDE-47 is highly persistent, toxic, and potentially bioaccumulative.[4,5] Its biomagnification in the food web and its presence in human and animal biological tissues, including breast milk, hair, semen, and placental tissues, have been associated with a high risk of certain symptoms of attention deficit hyperactivity disorder (ADHD) and socialization difficulties in postnatal children and may lead to impairments in neurobehavioral development, among other symptoms.[6,7] BDE-47 contamination is increasing globally in both freshwater and marine environments, posing a threat to aquatic organisms, particularly fish, and has the potential to spread along the food chain, ultimately affecting humans.[8] Therefore, developing a simple, lightweight, and cost-effective method for detecting BDE-47 in bodies of water is of great interest because detection can aid in selecting an appropriate method for the efficient removal of BDE-47 by determining its concentration.

Existing methods for detecting BDE-47 in water include liquid chromatography-mass spectrometry (LC-MS), high-performance liquid chromatography (HPLC), and gas chromatography-mass spectrometry (GC-MS).[9–12] However, current methods for testing BDE-47 are cumbersome and require expensive instruments and advanced technical skills.[13] Without solving the issue of concentration detection, selecting the most appropriate method for removing BDE-47, let alone achieving efficient remediation of BDE-47 contamination, is impossible. The development of a highly sensitive and straightforward method for BDE-47 detection is imperative and is the primary objective of this study. A successfully established method would provide a crucial methodological foundation for remediation studies, wherein accurate concentration measurements of BDE-47 are indispensable. Therefore, this study has significant potential applications.

[a]*School of Municipal and Geomatics Engineering, Hunan City University, Yiyang, Hunan 413000, China. E-mail: yuanpingli@hncu.edu.cn*

[b]*College of Environmental Science and Engineering, Hunan University, Key Laboratory of Environmental Biology and Pollution Control (Hunan University), Ministry of Education, Changsha 410082, China. E-mail: cyn@hnu.edu.cn*

† G. Zhang, Y. Li and S. Jia contributed equally to this work.

Furthermore, the use of sludge biochar as an electrode modifier for electrochemical detection of BDE-47 is relatively uncommon. Electrochemical detection offers inherent advantages over conventional organic detection methods in terms of portability, stability, ease of operation, rapid response, and low cost.[14] This detection method has been widely used for the efficient detection of substances such as metal ions, amino acids, and organic compounds.[15–17] Cyclic voltammetry (CV) is an electrochemical method, based on the interaction between electrode surfaces and ions, and serves as an important tool for studying the reduction and oxidation processes of molecular substances.[18] By measuring the electroactive surface area (ESA), CV reveals the kinetics and associated chemistry of thermodynamic redox processes and non-homogeneous phase electron transfer reactions and can be highly informative for reaction rate control diagnostics.[14,19]

Additionally, the preparation of effective electrochemically modified electrodes requires the selection of loading materials with a large specific surface area, good electrical conductivity, and excellent adsorption capacity.[20] Biochar is the solid residue produced by the thermal decomposition of various biological wastes under oxygen-limited conditions.[21] This residue is characterized by a porous structure, large specific surface area, high cation exchange capacity, excellent stability, and an abundance of surface functional groups. These properties make biochar an effective material for applications such as soil improvement, water treatment, and carbon sequestration.[22,23] Sludge is a by-product of the domestic wastewater treatment process and contains a variety of toxic organic and inorganic substances. These components can pose significant ecological risks to the environment and human health if not properly managed or treated.[24] Therefore, converting sewage sludge waste into value-added products, such as biochar, through thermochemical conversion in an oxygen-free environment can significantly reduce the leaching of inorganic and organic compounds into the aquatic environment. This process not only helps mitigate environmental pollution but also creates a valuable material with various applications in water purification, soil amendment, and energy production.[25,26] In particular, studying the reuse of sludge biochar is crucial to add value to it. Under the concept of converting waste into useful products, sludge biochar can be effectively repurposed as a renewable and readily available material for developing biomass-derived carbon materials.[27] This not only significantly reduces material costs, but also minimizes the leaching of heavy metals, organic pollutants, and pathogens from sludge products into soil and water, thereby promoting the resource utilization of sludge waste.[28] However, current biochar applications primarily focus on direct pollutant adsorption, with limited documented use in functionalized electrode modifications for contaminant concentration monitoring. Therefore, utilizing sludge biochar as a loading material for electrodes not only promotes the recycling of sludge but also mitigates the environmental hazards posed by the organic matter and heavy metals it contains, while enhancing the electrical conductivity of the working electrodes.[29]

Several modified electrodes have been reported for sensing POPs. As an example, Ahmad *et al.* constructed an enzyme-free electrochemical sensor (Ni(BPDC)MOF/GRP) based on a Ni-MOF for acetaminophen (AP) detection, which exhibited a wide linear response from 2.5 to 100 μM and a low detection limit of 0.056 μM, supporting fast and convenient monitoring. Nevertheless, the material preparation process did not facilitate the reuse of waste materials.[30] Li *et al.* developed a highly sensitive and efficient sensor for the detection of metronidazole (MNZ), which exhibited a wide linear detection range of 0.4–500 μM and a low detection limit of 0.25 μM. The sensor demonstrated excellent performance in detecting MNZ in complex samples such as honey and eggs. However, the preparation process of the modified material involved relatively complex procedures.[31] Quesada-González *et al.* employed screen-printed carbon electrodes (SPCEs) to detect polybrominated diphenyl ethers (PBDEs) in distilled water, attaining a detection limit of 21.5 ppb. This method enables rapid, sensitive, and low-cost monitoring of PBDE contaminants.[32] In the electrochemical detection of POPs, although existing modified electrodes can achieve low detection limits, their preparation processes are often complex, technically demanding, and costly, which restricts their practical application. In contrast, sludge biochar, obtained from waste resource utilization, offers distinct advantages, such as simple preparation and low cost. Sludge biochar is rich in diverse functional groups and has a well-developed pore structure. Using sludge biochar as an electrode modification material can not only simplify the electrode fabrication process effectively but also promote electron transfer and enrichment of target pollutants. This strategy has significant potential for achieving highly sensitive electrochemical detection based on a simple and low-cost preparation route. Therefore, the development of functionalized electrodes using sludge biochar exhibits considerable innovative potential and practical value for improving the detection efficiency and economic feasibility.

In this study, a simple strategy is proposed to convert municipal sludge into biochar using thermochemical methods. Different pyrolysis temperatures were tested to obtain sludge biochar with the optimal performance in all aspects. The data, including total pore volume, specific surface area, and pore size, were maximized at 600 °C, providing more adsorption sites for sludge biochar, as confirmed by SEM, BET, and FTIR analysis. The sludge biochar was then loaded onto an electrochemical working electrode using a thermal loading method and an adhesive to form an electrochemically modified electrode for detecting trace concentrations of BDE-47 in aqueous environments. The rapid, accurate, and easy detection of BDE-47 is a key component of the degradation process. Conventional detection methods for BDE-47 often rely on large and expensive testing equipment and complicated operational procedures. Therefore, the development and application of highly sensitive, compact, and cost-effective detection methods are expected to accelerate the advancement of BDE-47 degradation.

2. Materials and methods

2.1. Materials

Electrochemical measurements were performed using a CHI 660E electrochemical workstation (Shanghai Zhenhua Instrument Co., China). Material characterization was performed

using a MIRA3 field-emission scanning electron microscope (TESCAN, Czech Republic). A conventional three-electrode system comprising a 2.0 mm GCE working electrode (Shanghai Zhenhua), a Pt wire counter electrode (Shanghai Zhenhua), and a Ag/AgCl reference electrode (3 M KCl filling solution) was employed. Municipal sludge was obtained from the Tuanzhou Wastewater Plant in Yiyang City, Hunan Province. Material thermal treatment was conducted using an OTF-1200X tubular furnace (Hefei Kejing, China; max temp. 1200 °C) and a DZF-6050 vacuum drying oven (Shanghai Yiheng, China; vacuum to −0.098 MPa) for calcination and pre-drying, respectively.

A potassium ferricyanide solution was prepared using 5 mmol L^{-1} $K_3Fe(CN)_6$ and 100 mmol L^{-1} KCl solution as raw materials, maintaining a pH of 7 to serve as one supporting electrolyte. Phosphate-buffered saline (PBS) was prepared using 0.2 mol L^{-1} Na_2PO_4, 0.2 mol L^{-1} Na_2HPO_4, and 0.2 mol L^{-1} H_3PO_4 as raw materials to serve as another supporting electrolyte. The experimental solutions included 0.5 mol L^{-1} H_2SO_4 and 100 mg L^{-1} $CuSO_4$. The chemicals and materials used included *N*,*N*-dimethylformamide (DMF), alumina powder, sandpaper, H_3PO_4, and C_2H_6O. Deionized water was used in all the experiments.

2.2. Synthesis of sludge biochar

As demonstrated in Fig. 1, the sludge was divided into two portions: one was stored at 25 °C and the other at 4 °C. The material was washed several times with deionized water and dried at 105 °C for 24 h. Afterward, the material was washed again with deionized water and dried in a high-temperature drying oven at 105 °C for another 24 h. The dried material was crushed and placed in a quartz tube, which was then placed in a tube furnace and activated using a pyrolysis system. The samples were activated in an inert nitrogen (N_2) pyrolysis system and pyrolyzed in a muffle furnace at a heating rate of 10 °C min^{-1} to 400, 600, and 800 °C for 120 min. To remove the residual activation reagents, the products were washed with 10% HCl and neutralized with deionized water to achieve a pH of 7. The samples were dried in a vacuum oven at 105 °C for 12 h and stored in a desiccator until further use.

SEM was used to characterize the resulting sludge biochar samples, and FTIR spectroscopy was employed to determine the characteristics of the biochar pyrolyzed at different storage temperatures.

2.3. Preparation of the modified electrode

The specific production process is shown in Fig. 2. The surface of the reaction end of the GCE was first ground and polished, immersed in an ethanol solution, and ultrasonicated for 1 min. After cleaning, the electrode was placed in a 0.5 mol L^{-1} H_2SO_4. The cleaned electrode was then electrochemically treated using CV with a Ag/AgCl electrode as the reference electrode and a platinum electrode as the counter electrode, forming a three-electrode system, until the current stabilized during electrochemical treatment. Next, 5 mg of sludge biochar was dissolved in 1 mL of *N*,*N*-dimethylformamide (DMF), and the mixture was sonicated for 20 min. Then, 5 μL of the resulting solution was drop-coated onto the surface of GCE. The drop-coated GCE was subsequently dried in a vacuum oven at 115 °C for 15 min to complete the preparation.

2.4. Electrochemical detection of BDE-47

A three-electrode system was configured for CV measurements, comprising a sludge biochar-modified GCE (modified electrode) as the working electrode, a Ag/AgCl reference electrode, and a platinum counter electrode. CV was performed with the scanning cycle set to 4 and the potential swept between −0.3 V and +0.8 V. The modified electrode was first immersed in PBS containing BDE-47 for CV scanning to adsorb BDE-47. Subsequently, the BDE-47-adsorbed modified electrode was placed in a potassium ferricyanide solution (pH = 7) for another CV scanning, which yielded the CV scan diagram, and the peak current value was determined.

2.5. Parameter optimization of the pH

The experimental system maintained a constant concentration of BDE-47 solution (0.40 mg L^{-1}) in PBS across seven independent samples. The pH values of the samples were adjusted to 2, 3, 4, 5, 6, 7, and 8 using 98% concentrated phosphoric acid. Real-time monitoring of the peak current variations during successive scanning cycles enabled quantitative evaluation of the pH-dependent electrochemical response characteristics of

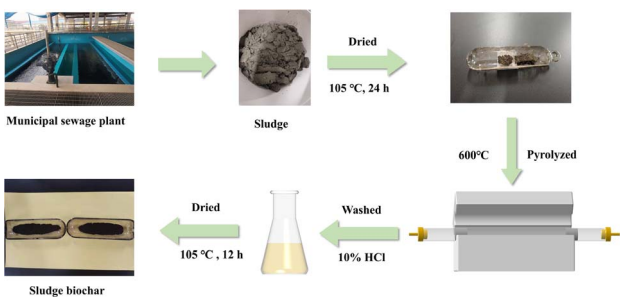

Fig. 1 Schematic illustration of the sludge biochar preparation process.

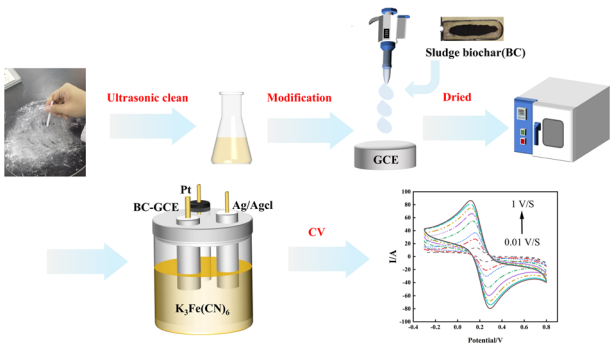

Fig. 2 Synthesis and sensing application of the modified electrode for trace BDE-47 detection.

the modified electrode. This protocol specifically investigates the correlation between solution acidity and signal transduction efficiency through a comparative analysis of redox current attenuation patterns.

2.6. Influence of the scanning rate

BDE-47 was added to PBS to maintain a sample concentration of 0.40 mg L^{-1} BDE-47 at a pH of 2.0. CV scanning was performed to confirm the successful adsorption of BDE-47 on the electrochemically modified electrode. Subsequently, the BDE-47 adsorbed electrochemical modified electrode was immersed in potassium ferricyanide solution, and scanning rates of 0.01 V s^{-1}, 0.05 V s^{-1}, 0.1 V s^{-1}, 0.3 V s^{-1}, 0.5 V s^{-1}, 0.7 V s^{-1}, 0.9 V s^{-1}, and 1 V s^{-1} were systematically applied to investigate the electrochemical behavior of BDE-47 at various scanning rates.

2.7. Interference experiment

Sodium ions (Na^+), potassium ions (K^+), calcium ions (Ca^{2+}), magnesium ions (Mg^{2+}), ferrous ions (Fe^{2+}), and lead ions (Pb^{2+}) at 100 times the concentration were added to PBS containing 0.20 mg L^{-1} BDE-47. Sulfate ions (SO_4^{2-}), chloride ions (Cl^-), glucose, citric acid, bisphenol A and phenol were also added to the PBS containing 0.20 mg L^{-1} BDE-47, ensuring that the concentration of each ion in the BDE-47 solution was 20 mg L^{-1}.

2.8. Construction of the BDE-47 linear detection curve

Based on these experimental results, the pH of the BDE-47 solution was adjusted to 2. Solutions with BDE-47 concentrations of 0.005 mg L^{-1}, 0.02 mg L^{-1}, 0.04 mg L^{-1}, 0.05 mg L^{-1}, 0.07 mg L^{-1}, 0.10 mg L^{-1}, 0.13 mg L^{-1}, 0.15 mg L^{-1}, 0.18 mg L^{-1}, 0.20 mg L^{-1}, 0.23 mg L^{-1}, 0.25 mg L^{-1}, 0.28 mg L^{-1}, 0.30 mg L^{-1}, 0.33 mg L^{-1}, 0.35 mg L^{-1}, 0.38 mg L^{-1}, 0.40 mg L^{-1}, 0.45 mg L^{-1}, 0.50 mg L^{-1}, 0.55 mg L^{-1}, and 0.60 mg L^{-1} were prepared. These concentrations were subjected to CV scanning, and the changes in the peak current were used to construct a linear curve for the accurate detection of trace BDE-47.

2.9. Recovery experiment

Seven water samples were collected from the Xiang River Basin, China (28°13′N, 112°96′E).

These water samples were pretreated using suction filtration. This involved assembling the extraction device with an appropriately trimmed filter membrane in a Brinell funnel. A tight seal was created by wetting a filter paper with distilled water. The operation of the pump enabled the sequential filtration of all water samples. The filtrates were then preserved in volumetric flasks for subsequent assays.

BDE-47 solutions of varying concentrations were added to PBS prepared with real water. The concentrations of the seven samples were adjusted to 50, 80, 200, 300, 400, 500, and 600 μg L^{-1}, respectively, and CV scanning was performed. Then, CV scanning was performed again using the novel electrochemically modified electrode in potassium ferricyanide solution to obtain the peak current values. The peak current values were substituted into a linear equation to determine the concentration of BDE-47. In addition, LC was used to validate the concentration of BDE-47 in PBS to ensure accuracy, and the electrochemical results were compared.

2.10. Stability of the modified electrode

The electrodes were placed in a constant temperature refrigerator at 4 °C and stored for 72 h. The electrodes were then removed, and CV scanning was performed. The temporal stability of the modified electrode was systematically evaluated through a quantitative comparison of the characteristic CV parameters before and after storage. This methodology enables the precise identification of performance degradation patterns in functional materials by analyzing critical indicators, including the redox peak current intensity, peak potential shift, and variations in the electroactive surface area.

3. Results and discussion

3.1. Characterization of sludge biochar

The morphology and structure of the sludge biochar pyrolyzed at 400, 600, 800 °C and 50k× image of biochar pyrolyzed at 600 °C are shown in Fig. 3. As the pyrolysis temperature increased, the surface structure of the sludge biochar gradually changed from fragmented to flat and smooth. The pore structure particles initially coalesced from a collapsed state, and the number of pores increased and became more concentrated. Table 1 presents the three-dimensional structure, pore volume, specific surface area, and average pore size parameters of sludge biochar prepared at different pyrolysis temperatures. The pore volume, specific surface area, and average pore diameter of the

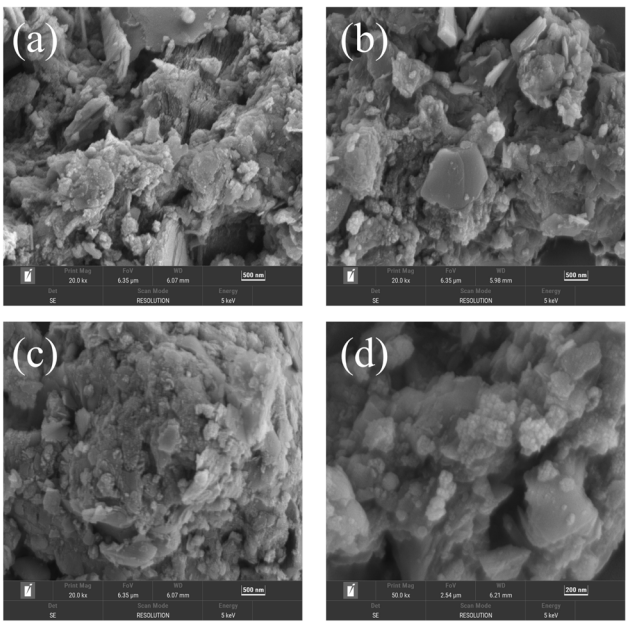

Fig. 3 20k× FESEM images of sludge biochar produced by pyrolysis at 400 °C, 600 °C, and 800 °C (a–c) and 50k× image of biochar pyrolyzed at 600 °C (d).

Table 1 Physicochemical parameters of sludge biochar prepared at pyrolysis temperatures. of 400 °C, 600 °C, 800 °C

Calcination temperature	Pore volume ($cm^3\ g^{-1}$) BJH		Specific surface area ($m^2\ g^{-1}$)	Total pore volume ($cm^3\ g^{-1}$) Single-point method		Average pore diameter (nm)	
	Adsorption	Desorption	BET	Adsorption	Desorption	Adsorption	Desorption
400 °C	0.104	0.095	35.654	0.070	0.086	7.854	9.752
600 °C	0.150	0.153	44.915	0.084	0.099	8.325	9.838
800 °C	0.125	0.130	52.904	0.071	0.089	5.399	6.735

sludge biochar prepared at a lower temperature (400 °C) were relatively small. At the medium temperature (600 °C), the three-dimensional structure of the sludge biochar became more pronounced. The pore volume increased from 0.104 $cm^3\ g^{-1}$ to 0.150 $cm^3\ g^{-1}$ in the adsorption state, the specific surface area increased from 35.654 $m^2\ g^{-1}$ to 44.915 $m^2\ g^{-1}$, and the average pore diameter changed from 7.854 nm to 8.325 nm (Table 1). This was attributed to the increase in pyrolysis temperature, which caused the pore structure to transition from collapsed to polymerized, forming more pore structures with additional adsorption sites. However, further increases in the pyrolysis temperature led to a higher degree of pore structure polymerization, resulting in the merging of different pore structures into a unified whole, causing the surface to become progressively smoother.[33,34] The total pore volume, specific surface area, and pore diameter of the sludge biochar prepared at 600 °C were larger than those of the biochars produced at other temperatures. Therefore, using sludge biochar prepared at 600 °C to construct an electrochemically modified electrode is more advantageous for improving the detection range and sensitivity.

The results of the FTIR characterization of sludge biochar, preserved at both 4 °C and 25 °C after pyrolysis at 600 °C, are presented in Fig. 4. Fig. 4 presents the FTIR spectrum, showing a peak at 477 cm^{-1} (O–O). Notably, the spectrum confirms the presence of a monosubstituted benzene ring, displaying the characteristic doublet of C–H out-of-plane bending vibrations at 796 cm^{-1} and 694 cm^{-1}. Furthermore, signals corresponding to C–O and O–H stretching vibrations were identified at 1046 cm^{-1} and 3382 cm^{-1}, respectively.[35,36] When compared to the sludge biochar preserved at ambient temperature, the biochar stored at 4 °C exhibited a reduction in the number of peaks near 3600 cm^{-1} and an overall decrease in transmittance. The observed differences in biochar FTIR characteristics can be traced to microbial-mediated alterations in the precursor composition during sludge storage at varying temperatures. When stored at 25 °C, sustained microbial metabolism profoundly degrades labile organic components, such as polysaccharides, which in turn influences the chemical pathways during pyrolysis.[37] In contrast, storage at 4 °C markedly inhibits microbial activity. Consequently, the reduced microbial degradation of labile organic components (*e.g.*, polysaccharides) in the precursors preserves their potential to form oxygen-containing functional groups (such as –C–O–C) during subsequent pyrolysis.[38] Studies have confirmed that the chemical composition of the biomass precursor plays a decisive role in defining the surface functional groups of the resulting biochar.[39] In particular, the transmittance of the –C–O–C peak at 1040 cm^{-1} showed a significant decline. Therefore, varying the storage temperature indirectly affected the surface chemical properties of biochar by regulating microbial activity and thus the composition of the raw materials. These findings indicate that the properties of sludge evolve over time under different preservation conditions and that the pyrolysis process influences the formation of functional groups.[25,40] Consequently, the electron transfer mechanisms observed when analyzing biochar from different sources may vary, reflecting the physicochemical differences in the functional groups.[27,41] The electron-donating ability is weakened because of the depletion of phenolic hydroxyl groups, thereby reducing the direct electron transfer capacity of the quinone/phenol redox couple (–C=O/–OH). The electronic conduction or shuttle effect of the aromatic carbon skeleton may be restructured because functional group degradation may alter the order of the carbon matrix. These physicochemical differences highlight the potential influence of the storage conditions on the electronic activity of biochar.[21,42]

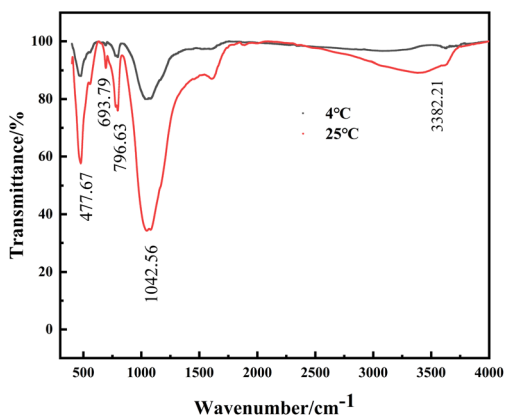

Fig. 4 Comparison of infrared spectra of sludge biochar stored at 4 °C and 25 °C.

3.2. Optimization of the pH

The influence of the solution pH on the peak current response is illustrated in Fig. 5. Starting at pH = 8, as the pH of the solution decreased, the acidity of PBS gradually increased, and the response peak current gradually increased, reaching

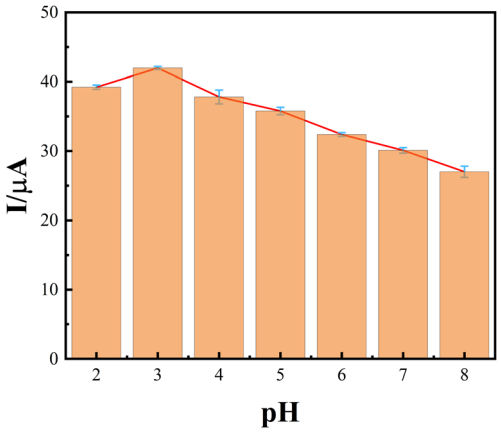

Fig. 5 Effect of the pH on the modified electrode.

a maximum at pH = 3. When the acidity of PBS continued to increase to pH = 2, the response peak current decreased. At lower pH values, the increase in protonation on the electrode drives more electrons to the electrode, resulting in higher current densities, which decrease as the pH value increases.[43] Notably, the sludge biochar-electrochemically modified electrode demonstrated superior performance under acidic conditions, achieving maximum current responses at pH = 3. The optimal performance under these low-pH conditions enhances the sensitivity of the modified electrode.[44,45] Therefore, the optimal pH for detection is 3.0. This facilitated the effective adsorption of BDE-47 and the accurate quantification of its concentration in aqueous solutions.

3.3. Influence of the scanning rate

As shown in Fig. 6, as the scanning rate increases, the current also increases. This suggests that the detection of BDE-47 is primarily controlled by its adsorption onto the surface of the modified electrode. Biochar efficiently enriches BDE-47 through nonspecific physical adsorption driven by hydrophobic effects and intermolecular forces, which is essentially a thermodynamically spontaneous process.[46–48] The rapid adsorption of BDE-47 is attributed to the large number of active adsorption sites on the surface of the biochar and the strong adsorption affinity between the adsorbate and the adsorbent. The organic functional groups in the biochar structure and their hydrophobic effects promote the adsorption of BDE-47. Additionally, pore diffusion is not the only rate-limiting step; membrane diffusion also participates in BDE-47 adsorption onto biochar.[49]

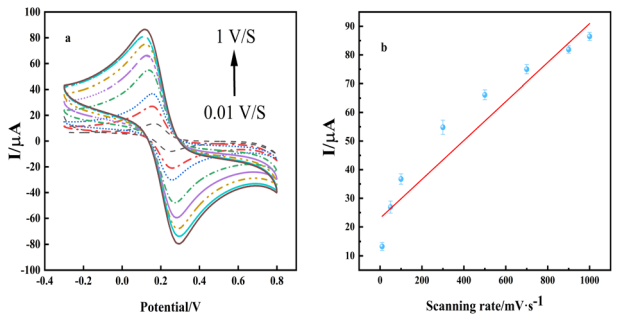

Fig. 6 CV curves of different scanning rates (a) and linear relationship plot between peak currents of BDE-47 *versus* scanning rates (b) (*vs.* Ag/AgCl reference electrode).

3.4. Interference experiment analysis

As shown in Fig. 7, the effects of Na^+, K^+, Ca^{2+}, Mg^{2+}, Fe^{2+}, Pb^{2+}, Cl^-, SO_4^{2-}, glucose, citric acid, bisphenol A, and phenol on the detection results resulted in a less than 10% change in the peak current, indicating that the sludge biochar modified electrode exhibited strong anti-interference properties. Alternatively, this may be due to the different functional groups and physicochemical properties of biochars derived from various raw materials. Sludge biochar physically adsorbs BDE-47, and specific functional groups on the biochar interact with the BDE-47 molecules. The π-structure of the BDE-47 molecule lacks electrons (π-electron acceptors) because the Br and ether groups in the BDE-47 molecule have strong electron-withdrawing properties, which can interact strongly with the electron-rich π-structure (π-electron donors) of the aromatic carbon domains in biochar.[50,51] The physical adsorption process occurs simultaneously, generating electrochemical signals. This adsorption mechanism enhances the preferential adsorption of BDE-47 by the sludge biochar. As more adsorption sites are occupied by BDE-47 molecules, fewer sites are available for the adsorption of heavy metal ions, leading to blocked pores and a reduced likelihood of heavy metal ion adsorption. Consequently, the presence of heavy metal ions did not interfere with the electrochemical detection of BDE-47 in water.

Therefore, using biochar for BDE-47 adsorption and detection through changes in the electrochemical signals during the adsorption process offers several advantages, including simplicity, low cost, high detection efficiency, and high accuracy. The method is highly resistant to interference from factors such as Na^+, K^+, Ca^{2+}, Mg^{2+}, Fe^{2+}, Pb^{2+}, Cl^-, SO_4^{2-}, glucose, citric acid, bisphenol A and phenol. This approach is important for the efficient detection of trace levels of BDE-47 in water, with high immunity to interference from various factors.

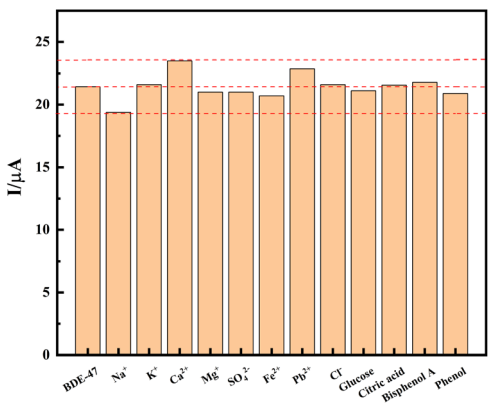

Fig. 7 Interference effects of coexisting substances on the peak currents.

3.5. Linear curve analysis of the electrochemically modified electrode

In a CV system, the electrochemical properties of the working electrode are compared with those of the reference electrode, and the counter electrode is placed in an electrolyte. Ferrocyanide redox pairs are commonly used to determine the electroactive surface area. The change in the redox peak current caused by electron transfer was used to construct a linear equation for BDE-47. By incorporating the peak current magnitude into this equation, the concentration of BDE-47 in water can be detected accurately and quickly without the need for cumbersome steps or expensive instrumentation. When the concentration of BDE-47 was in the range of 0.005–0.60 mg L^{-1}, electrochemical characterization showed that both the oxidation and reduction peak currents increased with increasing BDE-47 concentration and exhibited a good linear relationship,[52] as shown in Fig. 8.

A linear regression equation was constructed based on the relationship between the different concentrations of the BDE-47 standard solution and the change in the peak current, as shown in eqn (1). The correlation coefficient of the equation was $R^2 = 0.99$, indicating a strong linear relationship. The detection range was from 0.005 mg L^{-1} to 0.60 mg L^{-1}, with a lower limit of detection (LOD) of 5 ng L^{-1}.

$$\Delta I_{\text{BDE-47}} = 16.8125 \times (C_{\text{BDE-47}}) + 22.7186 \quad (1)$$

Moreover, differential pulse voltammetry (DPV) and square wave voltammetry (SWV) typically exhibit higher sensitivity for the quantitative analysis of trace substances because of their effective suppression of background currents.[53] Accordingly, in subsequent investigations, we will employ more sensitive techniques, such as DPV or SWV, to achieve lower detection limits, enhance the sensitivity for trace analysis, and thereby broaden the potential applications of the methodology.[54]

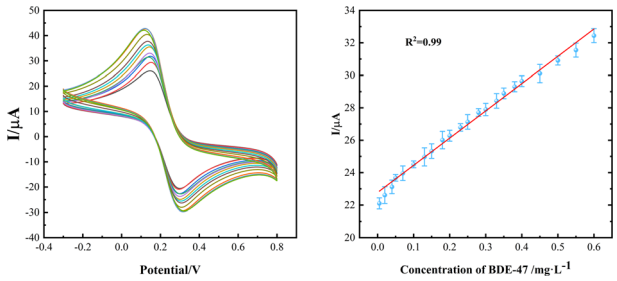

Fig. 8 Linear equation of BDE-47 (*vs.* Ag/AgCl reference electrode).

3.6. Analysis of actual water samples

The results of applying the electrochemical methods to the actual water samples are shown in Table 2. Compared to the results of the spiked recovery experiments of water samples using liquid chromatography, the recovery rate of this method ranged from 96.79% to 106.63%. These results are consistent with those obtained using traditional detection methods. The correlation analysis is shown in Fig. 9, where $R^2 = 0.998$. This indicates that the proposed method has good accuracy. However, because of the complex composition of actual water samples and their differences in composition, to improve the detection accuracy, performing qualitative analysis of the components in actual water samples and optimizing the experimental parameters is necessary. However, this electrochemical method shows great potential for the detection of trace amounts of heavy metals in water environments, particularly in acidic wastewater.[55] As presented in Table 3, the performance of the proposed method was evaluated against other electrochemical approaches and standard chromatographic techniques for the detection of PBDE congeners. The results demonstrate that, although this method provides a wider linear range than some existing techniques, its overall

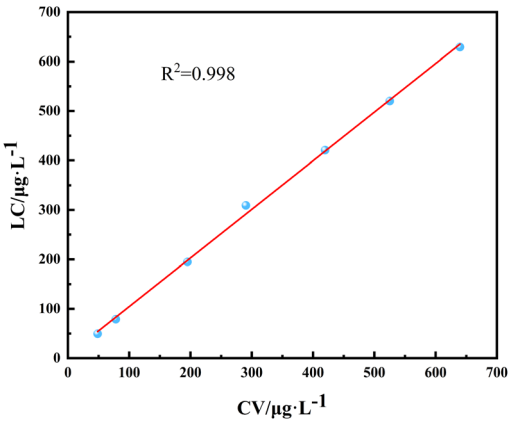

Fig. 9 Correlation analysis between liquid chromatography (LC) and cyclic voltammetry (CV) detection results.

Table 2 Comparative analysis of BDE-47 detection in four real samples: electrochemical method *vs.* liquid chromatography

		Detection concentration (μg L^{-1})		Recovery rate (%)	
	Actual concentration (μg L^{-1})	CV	Liquid chromatography	CV	Liquid chromatography
BDE-47	50	48.45	49.56	96.90	99.12
	80	78.21	78.98	97.76	98.72
	200	195.12	194.74	97.56	97.37
	300	290.36	309.19	96.79	103.06
	400	419.54	420.86	104.85	105.21
BDE-47	500	525.20	520.28	105.04	104.06
	600	639.78	629.32	106.63	104.88

Table 3 Comparative analysis of analytical techniques for PBDEs detection

Testing methods	Congeners	Limit of detection (LOD)	Linear range	Recovery	Ref.
CV	BDE-47	5 ng L^{-1}	0.005–0.60 mg L^{-1}	96.79% to 106.63%	This study
CV	BDE-15	0.14 μM	0.2∼8 μM	—	56
DPV	BDE-47	1.1 ng g^{-1}	—	—	57
DPV	BDE-47	0.18 ng mL^{-1}	0.30–6.9 ng mL^{-1}	—	58
Luminescence	BDE-209	0.01 μM	0.05–6.0 μM	—	59
Gas chromatography coupled with tandem mass spectrometry (GC-MS/MS)	BDE-47	2 ng L^{-1}	—	—	60
Gas chromatography coupled with triple quadrupole mass spectrometry (GC-MS/MS)	BDE-47	10.0 pg g^{-1}	0.20–10.0 ng m^{-1}	85.2% to 105.7%	61
Gas chromatography and mass spectrometry (GC-MS)	BDE-47	0.0023 ng mL^{-1}	—	—	62

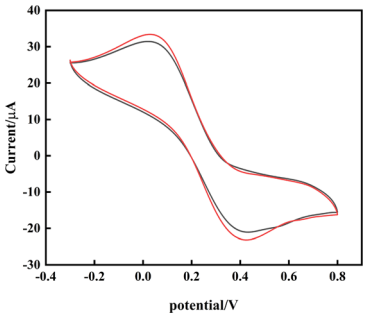

Fig. 10 Comparison of cyclic voltammetry scanning of the modified electrode before and after use (*vs.* Ag/AgCl reference electrode).

sensitivity remains lower than that of GC-MS. Nevertheless, its key strengths include cost efficiency, a short analysis time, and suitability for on-site monitoring, rather than serving as a replacement for established high-precision laboratory methods.

3.7. Stability of the electrochemically modified electrode

As demonstrated in Fig. 10, both freshly prepared and 72 h-used modified electrodes exhibited minimal variation in peak current responses, with the voltammetric curves remaining remarkably consistent. This observation confirms the structural stability of the sludge biochar immobilized on the glassy carbon electrode. Furthermore, the modified electrode retained >95% of its initial response amplitude after storage at 4 °C and repeated electrochemical measurements over a 72 h period, demonstrating excellent operational stability. These findings validate the reliability of the modified electrode for extended analytical applications that require multicycle detection of BDE-47.

4. Conclusion

In this study, a three-electrode detection system and analytical method were developed by loading sludge biochar onto a glassy carbon electrode. Municipal sludge was pyrolyzed into biochar at 600 °C, and the surface morphology was analyzed using FESEM, BET and FTIR spectroscopy. This process increased the surface area and pore volume of biochar, significantly enhancing the number of electrochemical reaction sites and improving the precision of the electrochemical detection of organic matter. The scanning rate and pH of the substrate during detection were optimized and examined, with pH 3 being the optimal condition for detecting BDE-47 in water using CV. The adsorption of BDE-47 onto the modified electrode was physical. Under these optimized conditions, standard curves for the qualitative and quantitative detection of BDE-47 were established. The modified electrode exhibited a wide detection range, capable of detecting trace BDE-47 over three orders of magnitude, from 0.005 to 0.60 mg L^{-1}, with a lower limit of detection (LOD) of 5 ng L^{-1} and recoveries ranging from 96.79% to 106.63%. Furthermore, the novel electrochemically modified electrode was used to detect BDE-47 in real water samples, and the results were consistent with those obtained using liquid chromatography.

In summary, the rapid, accurate, and convenient detection of BDE-47 is crucial. Traditional organic matter detection methods are often characterized by large and expensive equipment, high operational and maintenance costs, and complicated sample pretreatment processes. Additionally, most of these methods require timely pretreatment, which makes immediately analyzing the specific organic content in samples challenging, thus hindering real-time online detection. Without the accurate detection of BDE-47 concentrations, efficiently removing BDE-47 is difficult. In contrast, the new electrochemically modified electrode enables the rapid, efficient, real-time, and online detection of trace organics in a water environment. Its high sensitivity, specificity, and miniaturized design make it easy to operate and offer significant advantages over traditional methods.

Author contributions

Ganquan Zhang: investigation, writing – original draft, writing – review & editing. Yuanping Li: conceptualization, funding acquisition, project administration, writing – review & editing, supervision. Shunyao Jia: software, visualization, validation. Yaoning Chen: funding acquisition, project administration,

supervision. Tianyun Zhou: investigation, visualization, validation. Li Zhu: investigation, visualization. Nianping Chi: resources. Yanting Wu: visualization. Nqiang Luo: software.

Conflicts of interest

The authors declare that they have no conflict of interest.

Data availability

The data that support the findings of this study are available from the corresponding author upon reasonable request.

Acknowledgements

This study was financially supported by the National Natural Science Foundation of China (42477020), the Research Foundation of Education Department of Hunan Province (24A0578), the Innovation Training Program for College Students of Hunan Province (S202511527042), the Natural Science Foundation of Hunan Province, China (2023JJ30130), and the Engineering and Technology Centre for Safeguarding Drinking Water Quality in Hunan Villages and Towns Project (2019TP2079).

References

1 K. Huang, H. Liu, J. He, Y. He, X. Tao, H. Yin, Z. Dang and G. Lu, *J. Environ. Chem. Eng.*, 2021, **9**, 105077, DOI: 10.1016/j.jece.2021.105077.
2 A. Qadeer, S. Mubeen, M. Liu, T. G. Bekele, C. R. Ohoro, A. O. Adeniji, A. M. Alraih, Z. Ajmal, A. S. Alshammari, Y. Al-Hadeethi, D. Archundia, S. Yuan, X. Jiang, S. Wang, X. Li and S. Sauvé, *J. Hazard. Mater.*, 2024, **466**, 133543, DOI: 10.1016/j.jhazmat.2024.133543.
3 M. Kim and J. Han, *J. Water Process Eng.*, 2024, **63**, 105463, DOI: 10.1016/j.jwpe.2024.105463.
4 Y. Shi, X. Wei, Z. Zhang, S. Wang, H. Liu, D. Cui, W. Hua, Y. Fu, Y. Chen, Z. Xue, X. Li and W. Wang, *Aquat. Toxicol.*, 2024, **271**, 106933, DOI: 10.1016/j.aquatox.2024.106933.
5 M. Jin, J. Guo, Z. Xu, L. Sun and S. Zhang, *Atmos. Environ.*, 2025, **342**, 120906, DOI: 10.1016/j.atmosenv.2024.120906.
6 R. Henry, R. Vander Heide and N. M. Roy, *Environ. Toxicol. Pharmacol.*, 2025, **114**, 104627, DOI: 10.1016/j.etap.2025.104627.
7 Y. Chen, S. Ma, Y. Li, M. Yan, G. Zeng, J. Zhang, J. Zhang and X. Tan, *Appl. Microbiol. Biotechnol.*, 2016, **100**, 9709–9718, DOI: 10.1007/s00253-016-7798-8.
8 X. Zhang, Y. Huang, L. Yang, S. Chen, Y. Liu, N. Tang, Z. Li, X. Zhang, L. Li and D. Chen, *Ecotoxicol. Environ. Saf.*, 2024, **274**, 116192, DOI: 10.1016/j.ecoenv.2024.116192.
9 F. Ji, J. Wei, H. Luan, M. Li and Z. Cai, *Ecotoxicol. Environ. Saf.*, 2019, **184**, 109606, DOI: 10.1016/j.ecoenv.2019.109606.
10 J. Sha, Y. Wang, J. Lv, H. Wang, H. Chen, L. Qi and X. Tang, *J. Environ. Sci.*, 2015, **28**, 54–63, DOI: 10.1016/j.jes.2014.07.020.
11 C. A. Erratico, S. C. Moffatt and S. M. Bandiera, *Toxicol. Sci.*, 2011, **123**, 37–47, DOI: 10.1093/toxsci/kfr155.
12 J. Xin, X. Liu, L. Jiang and M. Li, *Chemosphere*, 2012, **87**, 477–482, DOI: 10.1016/j.chemosphere.2011.12.034.
13 U.-J. Kim and B. C. Kim, *Sens. Actuators, B*, 2017, **248**, 298–304, DOI: 10.1016/j.snb.2017.03.139.
14 C.-M. Chou, Y.-D. Dai, C. Yuan and Y.-H. Shen, *Environ. Res.*, 2023, **236**, 116785, DOI: 10.1016/j.envres.2023.116785.
15 Y. Liu, Y. Deng, H. Dong, K. Liu and N. He, *Sci. China: Chem.*, 2017, **60**, 329–337, DOI: 10.1007/s11426-016-0253-2.
16 M. Mehdi Foroughi, S. Jahani and S. Rashidi, *Microchem. J.*, 2024, **198**, 110156, DOI: 10.1016/j.microc.2024.110156.
17 N. Walpen, M. H. Schroth and M. Sander, *Environ. Sci. Technol.*, 2016, **50**, 6423–6432, DOI: 10.1021/acs.est.6b01120.
18 Y. Ma, X.-L. Shen, Q. Zeng, H.-S. Wang and L.-S. Wang, *Talanta*, 2017, **164**, 121–127, DOI: 10.1016/j.talanta.2016.11.043.
19 S. Y. Vassiliev, V. V. Sentyurin, E. E. Levin and V. A. Nikitina, *Electrochim. Acta*, 2019, **302**, 316–326, DOI: 10.1016/j.electacta.2019.02.043.
20 Y. Li, H. Wang, B. Yan and H. Zhang, *J. Electroanal. Chem.*, 2017, **805**, 39–46, DOI: 10.1016/j.jelechem.2017.10.022.
21 Y. Chen, M. Zhao, Y. Li, Y. Liu, L. Chen, H. Jiang, H. Li, Y. Chen, H. Yan, S. Hou and L. Jiang, *J. Environ. Manage.*, 2023, **344**, 118497, DOI: 10.1016/j.jenvman.2023.118497.
22 Y. Liu, M. Zhao, Y. Chen, Y. Li, H. Jiang, L. Chen, L. Jiang, H. Li, Y. Chen and S. Hou, *Sep. Purif. Technol.*, 2024, **346**, 127499, DOI: 10.1016/j.seppur.2024.127499.
23 Y. Liu, Y. Chen, Y. Li, L. Chen, H. Jiang, M. Zhao, H. Li, C. Zhao, H. Kang and W. Zhou, *Sci. Total Environ.*, 2024, **920**, 170803, DOI: 10.1016/j.scitotenv.2024.170803.
24 Y. Chen, F. Xu, H. Li, Y. Li, Y. Liu, Y. Chen, M. Li, L. Li, H. Jiang and L. Chen, *J. Anal. Appl. Pyrolysis*, 2021, **156**, 105173, DOI: 10.1016/j.jaap.2021.105173.
25 Y. Li, M. Zhao, H. Yan, Y. Chen, Y. Liu, H. Jiang, L. Chen, S. Hou, N. Chi and S. Jia, *J. Water Process Eng.*, 2024, **60**, 105218, DOI: 10.1016/j.jwpe.2024.105218.
26 W. D. Chanaka Udayanga, A. Veksha, A. Giannis, G. Lisak and T.-T. Lim, *Energy Convers. Manage.*, 2019, **196**, 1410–1419, DOI: 10.1016/j.enconman.2019.06.025.
27 Y. Li, Y. Liu, Y. Liu, Y. Chen, L. Chen, H. Yan, Y. Chen, F. Xu, M. Li and L. Li, *J. Water Process Eng.*, 2022, **48**, 102864, DOI: 10.1016/j.jwpe.2022.102864.
28 Y. Jiang, X. Sun, H. Zhang, Q. Li, J. Mo, M. Xing, B. Dong and H. Zhu, *Sustainability*, 2024, **16**, 5667, DOI: 10.3390/su16135667.
29 S. Singh, V. Kumar, D. S. Dhanjal, S. Datta, D. Bhatia, J. Dhiman, J. Samuel, R. Prasad and J. Singh, *J. Cleaner Prod.*, 2020, **269**, 122259, DOI: 10.1016/j.jclepro.2020.122259.
30 M. W. Ahmad, J. Y. Al-Humaidi, K. S. Kushwaha, B. Dey, A. Choudhury, A. Albishri and M. M. Rahman, *Mater. Sci. Semicond. Process.*, 2026, **201**, 110031, DOI: 10.1016/j.mssp.2025.110031.
31 Y.-Y. Li, F. Guo, J. Yang and J.-F. Ma, *Food Chem.*, 2023, **425**, 136482, DOI: 10.1016/j.foodchem.2023.136482.
32 D. Quesada-González, A. Baiocco, A. A. Martos, A. de la Escosura-Muñiz, G. Palleschi and A. Merkoçi, *Biosens.*

Bioelectron., 2019, **127**, 150–154, DOI: **10.1016/j.bios.2018.11.050**.
33 Y. Chen, X. Luo, Y. Li, Y. Liu, L. Chen, H. Jiang, Y. Chen, X. Qin, P. Tang and H. Yan, *Chemosphere*, 2022, **301**, 134563, DOI: **10.1016/j.chemosphere.2022.134563**.
34 Y. Liu, Y. Chen, Y. Li, L. Chen, H. Jiang, H. Li, X. Luo, P. Tang, H. Yan, M. Zhao, Y. Yuan and S. Hou, *J. Hazard. Mater.*, 2022, **431**, 128584, DOI: **10.1016/j.jhazmat.2022.128584**.
35 E. Inbar and A. Arie, *Appl. Phys. B*, 1999, **68**, 99–105, DOI: **10.1007/s003400050593**.
36 H. Choi, X. Liu, G. Gonzalez Abad, J. Seo, K.-M. Lee and J. Kim, *Remote Sens.*, 2021, **13**, 152, DOI: **10.3390/rs13010152**.
37 Y. Yan, X. Li, K. Yu, Z. Wu, Y. Sun, Z. Cheng, B. Zhao, C. Nie and Y. Xia, *Environ. Pollut.*, 2024, **343**, 123283, DOI: **10.1016/j.envpol.2023.123283**.
38 K. L. S. Duarte, R. M. Castellanos, R. C. Costa, C. F. Mahler and J. P. Bassin, *J. Environ. Manage.*, 2021, **296**, 113200, DOI: **10.1016/j.jenvman.2021.113200**.
39 M. Hassan, Y. Liu, R. Naidu, S. J. Parikh, J. Du, F. Qi and I. R. Willett, *Sci. Total Environ.*, 2020, **744**, 140714, DOI: **10.1016/j.scitotenv.2020.140714**.
40 C. Liu, H. Li, J.-Q. Ni, G. Zhuo, W. Chen, Y. Zheng and G. Zhen, *Sci. Total Environ.*, 2024, **906**, 167816, DOI: **10.1016/j.scitotenv.2023.167816**.
41 Y. Yang, Z. Song, W. Ren, J. Vongsvivut, Z. Wang, N. Ren, X. Duan and Y. Chen, *Appl. Catal., B*, 2024, **359**, 124470, DOI: **10.1016/j.apcatb.2024.124470**.
42 Y. Chen, W. Zhou, Y. Li, H. Kang, M. Zhao, Y. Liu, J. Wang, C. Zhao, B. Zou, X. Jia and W. Zhang, *J. Colloid Interface Sci.*, 2025, **686**, 471–486, DOI: **10.1016/j.jcis.2025.01.156**.
43 A. M. Manoj and L. R. Viannie, *J. Solid State Electrochem.*, 2025, **29**, 107–116, DOI: **10.1007/s10008-024-06078-z**.
44 S. Jia, Y. Li, Y. Chen, Y. Wu, T. Zhou, N. Chi, G. He, W. Zhang, W. Luo, H. Li and Y. Deng, *RSC Adv.*, 2025, **15**, 17535–17547, DOI: **10.1039/d5ra02612a**.
45 L. Li, N. Limani, R. P Antony, S. Dieckhöfer, C. Santana Santos and W. Schuhmann, *Small Sci.*, 2024, **4**, 2300283, DOI: **10.1002/smsc.202300283**.
46 G. Liu, H. Sheng, Y. Fu, Y. Song, M. Redmile-Gordon, Y. Qiao, C. Gu, L. Xiang and F. Wang, *Chemosphere*, 2019, **214**, 176–183, DOI: **10.1016/j.chemosphere.2018.09.081**.
47 Y. Yan, W. Ma, Y. Zhang, C. Nie, H. Guo and X. Lun, *Desalin. Water Treat.*, 2016, **57**, 29328–29339, DOI: **10.1080/19443994.2016.1169221**.
48 R. Qi, C. Qian, Y. Li and Y. Wang, *Environ. Pollut.*, 2024, **361**, 124779, DOI: **10.1016/j.envpol.2024.124779**.
49 G. Liu, Y. Song, H. Sheng, M. Ye, R. D. Stedtfeld, Y. Bian, C. Gu, X. Jiang and F. Wang, *Pedosphere*, 2019, **29**, 721–729, DOI: **10.1016/S1002-0160(18)60063-3**.
50 J. Xin, R. Liu, H. Fan, M. Wang, M. Li and X. Liu, *J. Environ. Sci.*, 2013, **25**, 1368–1378, DOI: **10.1016/S1001-0742(12)60222-8**.
51 X. Qi, H. Yin, M. Zhu, P. Shao and Z. Dang, *Water Res.*, 2022, **220**, 118679, DOI: **10.1016/j.watres.2022.118679**.
52 K. Qu, X. Hu and Q. Li, *Diamond Relat. Mater.*, 2023, **131**, 109617, DOI: **10.1016/j.diamond.2022.109617**.
53 M. Faisal, J. Ahmed, M. M. Alam, M. Alsaiari, A. M. Asiri, R. H. Althomali, F. A. Harraz and M. M. Rahman, *Microchem. J.*, 2024, **200**, 110295, DOI: **10.1016/j.microc.2024.110295**.
54 A. Çağıl, G. Doğan and A. Levent, *J. Food Compos. Anal.*, 2025, **139**, 107070, DOI: **10.1016/j.jfca.2024.107070**.
55 C. S. Ong, Q. H. Ng, A. L. Ahmad and S. C. Low, *Anal. Chim. Acta*, 2025, **1335**, 343423, DOI: **10.1016/j.aca.2024.343423**.
56 X. Jiang, X. Bai, X. Liu, X. Wang and K.-K. Shiu, *Sens. Diagn.*, 2023, **2**, 176–187, DOI: **10.1039/D2SD00161F**.
57 S. Romanelli, F. Bettazzi, T. Martellini, W. L. Shelver, A. Cincinelli, R. Galarini and I. Palchetti, *Talanta*, 2017, **170**, 540–545, DOI: **10.1016/j.talanta.2017.04.027**.
58 F. Bettazzi, T. Martellini, W. L. Shelver, A. Cincinelli, E. Lanciotti and I. Palchetti, *Electroanalysis*, 2016, **28**, 1817–1823, DOI: **10.1002/elan.201600127**.
59 X. Chen, H. Yao, D. Song, G. Sun and M. Xu, *Chem. Eng. J.*, 2022, **433**, 133266, DOI: **10.1016/j.cej.2021.133266**.
60 M. Liu, X. Jia, R. Peng, Z. Bai, J. Yuan and L. Tan, *J. Sep. Sci.*, 2024, **47**, e70010, DOI: **10.1002/jssc.70010**.
61 X. Li, R. Yang, Z. Bai, P. Gan, T. Zeng, M. Liu and J. Yuan, *Food Chem.*, 2025, **467**, 142361, DOI: **10.1016/j.foodchem.2024.142361**.
62 C. M. Bustamanste, P. Ruiz, A. B. Rifat, N. Bravo, J. O. Grimalt and M. Garí, *J. Chromatogr. A*, 2025, **1759**, 466235, DOI: **10.1016/j.chroma.2025.466235**.